Communications in Physics, Vol. 14, No. 2 (2004), pp. 74 – 83

ANHARMONIC EXAFS AND ITS PARAMETERS OF HCP CRYSTALS: THEORY AND COMPARISON TO EXPERIMENT

NGUYEN VAN HUNG AND DAO XUAN VIET

Department of Physics, College of Natural Sciences,

Hanoi National University

Abstract. *A new theory for ab initio calculation of the anharmonic Extended X-ray Absorption Fine Structure (EXAFS) and its parameters of hcp crystals has been developed based on the single- shell model. Analytical expressions for the anharmonic contributions to the amplitude and to the phase of EXAFS and a new anharmonic factor have been derived. The EXAFS cumulant expressions are formulated based on the anharmonic correlated Einstein model. The EXAFS function and its parameters contain anharmonic effects at high temperature and appoach those of the harmonic model at low temperature. Numerical results for Zn agree well with the experimental values.*

I. INTRODUCTION

The harmonic EXAFS ab initio calculation method [1] works very well at low temperatures because the anharmonic contributions to the atomic thermal vibrations can be neglected. But at different high temperatures the EXAFS spectra provide apparently different structural information [2-19] (Fig. 1) due to the anharmonicity, and these effects need to be evaluated.

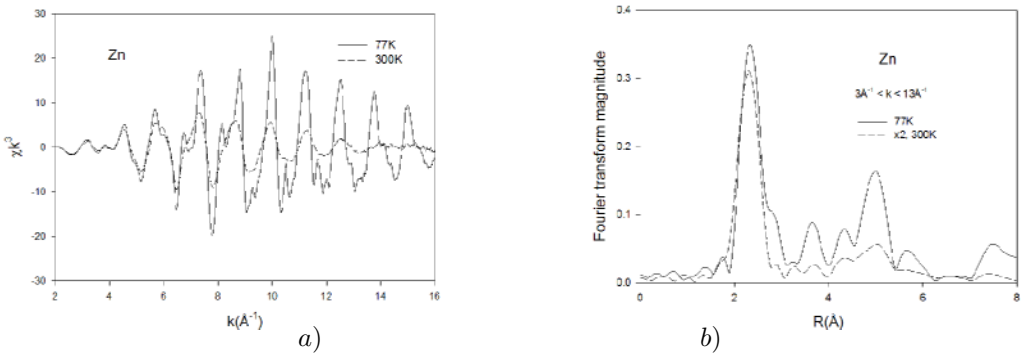

a) *b)*

Fig. 1. EXAF spectra χk^3 (a) and their Fourier transform magnitudes (b) of Zn at 77 K (solid) and 300 K (dash) measured at HASYLAB am SESY, Germany [16].

The formalism for including anharmonic effects in EXAFS is often based on the cumulant expansion approach [3,4], and the anharmonic effects in EXAFS have been valuated by the ratio methods [3-9] in which the EXAFS and their Fourier transform magnitudes at two different temperatures are compared to deduce the anharmonic effects in EXAFS. Some progresses have been done towards ab initio calculation of EXAFS including anharmonic contributions [10-14] either by an empirical procedure [10-13] or by an analytical procedure [14] for fcc crystals.

The purpose of this work is to develop a new theory for ab initio calculation of EXAFS including anharmonic contributions of hcp crystals by deriving analytical expressions for the anharmonic contributions to the amplitude and to the phase of the EXAFS.

A new anharmonic factor has been developed to determine the anharmonic contribution to the amplitude. To calculate the cumulants contained in the derived expressions the quantum statistical approach with anharmonic correlated Einstein model [13] has been used in which the parameters of the anharmonic effective potential are based on our calculated Morse potential that characterizes the interaction between each pair of atoms, and the anharmonicity is described by the cumulants obtained by the calculation of the phonon-phonon interaction process [13,19]. Numerical results for Zn are discussed and are found to be in good agreement with the experimental data [16].

II. FORMALISM

According to the cumulant expansion approach the EXAFS oscillation function is given by

$$\chi(k) = F(k)\frac{e^{-2R/\lambda(k)}}{kR^2} Im\left\{e^{i\Phi(k)}\exp\left[2ikR + \sum_n \frac{(2ik)^n}{n!}\sigma^{(n)}\right]\right\}, \tag{1}$$

where $F(k)$ is the real atomic backscattering amplitude,Φ is the net phase shift, k and λ are the wave number and the mean free path of the photoelectron, respectively, and $\sigma^{(n)}$ (n = 1,2,3, ...) are the cumulants. They appear due to the thermal average of the function $\exp(i2kr)$ in which the asymmetric terms are expanded in a Taylor series about $R = \langle r\rangle$ with r as the instantaneous bond length between absorbing and backscattering atoms and then are rewritten in terms of cumulants.

This EXAFS oscillation function including anharmonic effects contains the Debye-Waller factor $e^{-W(k,T)}$ accounting for the effects of the thermal vibrations of atoms. Based on the analysis [3-5,13] of cumulant expansion we obtain

$$\begin{aligned} W(k,T) =& 2ik\sigma^{(1)}(T) - 2k^2\sigma^{(2)}(T) - 4ik\sigma^{(2)}(T)\left(\frac{1}{R}+\frac{1}{\lambda(k)}\right) \\ &- \frac{4}{3}ik^3\sigma^{(3)}(T) + \frac{2}{3}\sigma^{(4)}(T)k^4 + \cdots \end{aligned} \tag{2}$$

where $\sigma^{(1)}$ is the first cumulant or net thermal expansion; $\sigma^{(2)}$ is the second cumulant which is equal to the mean square relative displacement (MSRD) or Debye-Waller factor σ^2; $\sigma^{(3)}$ and $\sigma^{(4)}$ are the third and the fourth cumulants, respectively. The higher cumulants are not included due to their small contributions [9,13,14,18].

To consider anharmonic contributions to the MSRD we used an argument analogous to the one [20] for its change due to the temperature increase and obtain

$$\sigma^2(T) - \sigma^2(T_o) = (1+\beta(T))\left[\sigma_H^2(T) - \sigma^2(T_o)\right], \quad \beta(T) = 2\gamma_G\frac{\Delta V}{V}, \tag{3}$$

where γ_G is Grüneisen parameter, and $\Delta V/V$ is the relative volume change due to thermal expansion,T_o is a very low temperature so that $\sigma^2(T_o)$ is a harmonic MSRD. This result agrees well with the one in another consideration [5] on the change of the MSRD. Deriving further Eq. (3) we obtain the total MSRD

$$\sigma^2(T) = \sigma_H^2(T) + \beta(T)\left[\sigma_H^2(T) - \sigma^2(T_o)\right]. \tag{4}$$

It is clear that the MSRD approaches the very small value of zero-point contribution σ_0^2 when the temperature approaches zero, i. e.,

$$\sigma^2(T_o) \to \sigma_0^2 \ for\ T_o \to 0. \tag{5}$$

Hence, it can be seen in Eq. (4) that the total MSRD $\sigma^2(T)$ at a given temperature T consists of the harmonic $\sigma_H^2(T)$ and the anharmonic $\sigma_A^2(T)$ contributions

$$\sigma^2(T) = \sigma_H^2(T) + \sigma_A^2(T)\ , \quad \sigma_A^2 = \beta(T)\left[\sigma_H^2(T) - \sigma_0^2\right]. \tag{6}$$

This separation will help us to determine the anharmonic contributions to the EXAFS amplitude.

The anharmonic correlated Einstein model [13] is now used widly in EXAFS data analysis [14,15,17,22-27]. In the present approach we apply this theory to the calculation of the cumulants where the effective interaction potential is given by

$$V_{eff}(x) \cong \frac{1}{2}k_{eff}x^2 + k_3x^3 + \cdots = V(x) + \sum_{j\neq i} V\left(\frac{\mu}{M_i}x\hat{\mathbf{R}}_{12}.\hat{\mathbf{R}}_{ij}\right), \mu = \frac{M_1M_2}{M_1+M_2}. \tag{7}$$

Here x is the deviation of instantaneous bond length between two atoms from equilibrium, $\hat{\mathbf{R}}$ is the bond unit vector, k_{eff} is effective spring constant, and k_3 the cubic parameter giving an asymmetry in the pair distribution function. The correlated Einstein model may be defined as a oscillation of a pair of atoms with masses M_1 and M_2 (e.g., absorber and backscatterer) in a given system. Their oscillation is influenced by their neighbors given by the last term in the left hand side of Eq. (7), where the sum i is over absorber ($i = 1$) and backscatterer ($i = 2$), and the sum j is over all their nearest neighbors, excluding the absorber and backscatterer themselves whose contributions are described by the term $V(x)$.

To model the asymmetry we replaced the harmonic potential by an anharmonic one, e. g., a Morse potential expanded only to the third order due to small anharmonicity in EXAFS

$$V(x) = D\left(e^{-2\alpha x} - 2e^{-\alpha x}\right) \cong D\left(-1 + \alpha^2x^2 - \alpha^3x^3 + \cdots\right), \tag{8}$$

where x is the deviation of instantaneous bond length between the two atoms from equilibrium, D is disociation energy and *1/*α corresponds to the width of the potential.

Applying Eq. (8) to the effective potential of the system of Eq. (7) (ignoring the overall constant) we obtain

$$k_{eff} = 5D\alpha^2\left(1 - \frac{3}{2}\alpha\, a\right) = \mu\,\omega_E^2;\ \ k_3 = -\frac{5}{4}D\alpha^3;\quad \theta_E = \frac{\hbar\omega_E}{k_B}, \tag{9}$$

where k_B is Boltzmann constant; ω_E ,θ_E are the correlated Einstein frequency and temperature, respectively.

We use the definition [13,19] $y = x - a$ as the deviation from the equilibrium value of x at temperature T to rewrite Eq. (7) as the sum of the harmonic contribution

and a perturbation δV due to the weak anharmonicity (ignoring the overall constant for convenience)

$$V_{eff}(y) = \frac{1}{2}k_{eff}y^2 + \delta V(y), \quad \delta V(y) = 5D\alpha^2\left(ay - \frac{1}{4}\alpha y^3\right). \tag{10}$$

To use phonon-phonon interaction procedure in quantum statistics [21] we express y in terms of anihilation and creation operators, $\hat{a}$ and $\widehat{a}^+$, i. e.,

$$y = \kappa\left(\hat{a} + \hat{a}^+\right); \qquad \kappa^2 = \frac{\hbar}{2\mu\omega_E} \tag{11}$$

and use harmonic oscillator state $|n\rangle$ with eigenvalue $E_n = n\hbar\omega_E$(ignoring the zero point energy for convenience). The MSRD is described by

$$\sigma^2 = \frac{1}{Z}Tr\left(\rho\, y^2\right) = \frac{1}{Z}\sum_n e^{-n\beta\,\hbar\omega_E}\,\langle n|y^2|n\rangle, \tag{12}$$

where due to weak anharmonicity in EXAFS we neglected [19] the small perturbation $\delta\rho$ in the statistical density matrix $\rho = \rho_0 + \delta\rho$ so that the canonical partition function is given by

$$Z \approx Tr\rho_o = \sum_n e^{-n\beta\,\hbar\omega_E} = \sum_{n=0}^{\infty} z^n = \frac{1}{1-z}; \quad \beta = 1/k_BT. \tag{13}$$

For the odd cumulants (m = 1, 3, ...) we calculate

$$\langle y^m\rangle = \frac{1}{Z}Tr\left(\rho y^m\right) = \frac{1}{Z}\sum_{n,n'}\frac{e^{-\beta E_n} - e^{-\beta E'_n}}{E_n - E'_n}\,\langle n|\,\delta V_{eff}\,|n'\rangle\,\langle n'|\,y^m\,|n\rangle. \tag{14}$$

Using the above results in first-order thermodynamic perturbation theory with consideration of the phonon-phonon interaction for taking into account the anharmonicity we obtain the cumulants

$$\sigma^{(1)}(T) = \sigma_o^{(1)}\frac{1+z}{1-z} = \frac{3\alpha}{4}\sigma^2, \quad \sigma_o^{(1)} = \frac{3\alpha}{4}\sigma_o^2, \quad z = e^{-\theta_E/T}, \tag{15}$$

$$\sigma^2(T) = \sigma_o^2\frac{1+z}{1-z}, \qquad \sigma_o^2 = \frac{\hbar\omega_E}{10D\alpha^2}, \tag{16}$$

$$\sigma^{(3)}(T) = \sigma_o^3\frac{1+10z+z^2}{(1-z)^2}, \quad \sigma_o^{(3)} = \frac{\alpha}{2}\left(\sigma_o^2\right)^2, \tag{17}$$

where $\sigma_o^{(1)}$, σ_o^2, $\sigma_o^{(3)}$ are the zero-point contributions to the first, second and third cumulant, respectively.

Based on the derived cumulants and the correlated Einstein frequency we calculated the relative volume change due to thermal expansion $\Delta V/V$ and Grüneisen parameter γ_G. By substituting the obtained results in Eq. (3) we derived an anharmonic factor

$$\beta(T,R) = \frac{9\hbar\omega_E}{80D}\frac{1+z}{1-z}\left[1 + \frac{3\hbar\omega_E}{40D\alpha R}\frac{1+z}{1-z}\left(1 + \frac{\hbar\omega_E}{40D\alpha R}\frac{1+z}{1-z}\right)\right]. \tag{18}$$

This factor is proportional to the temperature and inversely proportional to the shell radius, thus reflecting a similar property of anharmonicity obtained in an experimental catalysis research [2] if R is considered as particle radius.

The anharmonic contribution to the EXAFS phase at a given temperature is the difference between the total phase and the one of the harmonic EXAFS. On the left hand side of Eq. (2) the 2^{nd} and the 5^{th} terms contribute to the EXAFS amplitude. Only the 1^{st}, the 4^{th} terms and the anharmonic contribution to the MSRD in the 3^{rd} term are anharmonic contributions to the phase. Therefore, from this equation we obtain

$$\Phi_A(T,k) = 2k\left[\sigma^{(1)}(T) - 2\sigma_A^2(T)\left(\frac{1}{R}+\frac{1}{\lambda(k)}\right) - \frac{2}{3}\sigma^{(3)}(T)k^2\right]. \tag{19}$$

The 4^{th} cumulant is often very small [9,13,14,18]. This is why we obtained from Eqs. (1, 2), taking into account the above results, the temperature dependent K-edge EXAFS function including anharmonic effects as

$$\chi(k,T) = \sum_j \frac{S_0^2 N_j}{kR_j^2} F_j(k)\, e^{-\left(2k^2\sigma^2(T)+2R_j/\lambda(k)\right)} \sin\left(2kR_j + \Phi_j(k) + \Phi_A^j(k,T)\right), \tag{20}$$

which by including Eq. (6) is resulting in

$$\chi(k,T) = \sum_j \frac{S_0^2 N_j}{kR_j^2} F_j(k) e^{-\left(2k^2\left[\sigma_H^2(T)+\sigma_A^2(T)\right]+2R_j/\lambda(k)\right)} \sin\left(2kR_j + \Phi_j(k) + \Phi_A^j(k,T)\right), \tag{21}$$

where S_0^2 is the square of the many body overlap term, N_j is the atomic number of each shell, the remaining parameters were defined above, the mean free path λ is defined by the imaginary part of the complex photoelectron momentum $p = k + i/\lambda$, and the sum is over all atomic shells.

It is obvious that in Eq. (21) $\sigma_A^2(T)$ determines the anharmonic contribution to the amplitude characterizing the attenuation, and $\Phi_A(k,T)$ is the anharmonic contribution to the phase characterizing the phase shift of EXAFS spectra. They are calculated by Eq. (6) and Eq. (19), respectively. Their values characterize the temperature dependence of the anharmonicity, but the anharmonicity is described by the cumulants given by Eqs. (15-17) obtained by consideration of the phonon-phonon interaction process. That is why they also characterize the temperature dependence of the phonon-phonon interaction in the EXAFS of hcp crystals. At low temperature these anharmonic values approach zero and the EXAFS function Eq. (21) is reduced to the one of the harmonic model.

III. DISCUSSION OF NUMERICAL RESULTS AND COMPARISON TO EXPERIMENT

Now we apply the expressions derived in the previous section to numerical calculations for hcp crystals. The Morse potential parameters D = 0.1688 eV, α = 1.7054 Å^{-1} for Zn and D = 0.1675 eV, α = 1.9069 Å^{-1} for Cd have been calculated using the procedure presented in [15]. Morse potential calculated for Zn is illustrated in Fig. 2 in

comparison to experiment [28]. These values are used for calculation of the EXAFS data. Fig. 2 shows the temperature dependence of our calculated anharmonic factors of Zn and Cd. Anharmonic factor of Zn is 3.75 % at 300 K, but only 0.28 % at 77 K. This figure also denotes that the anharmonic effect in Zn is stronger than the one in Cd. The temperature dependence of our calculated anharmonic contribution to EXAFS amplitude or to MSRD of Zn is illustrated in Fig. 4 in comparison to experiment [16]. Fig. 5 shows the temperature

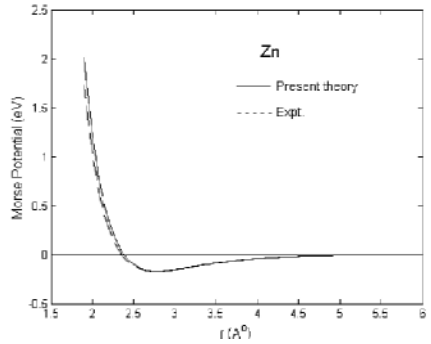

Fig. 2. Calculated Morse potential of Zn compared to experiment [28].

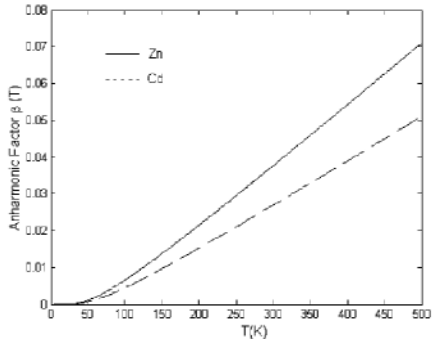

Fig. 3. Temperature dependence of calculated anharmonic factors of Zn and Cd

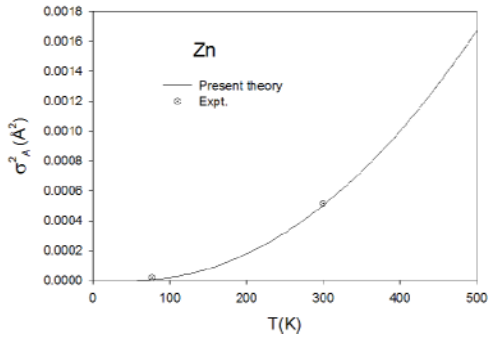

Fig. 4. Temperature dependence of the calculated anharmonic contribution of Zn to MSRD or to EXAFS amplitude in comparison to experimental values [16].

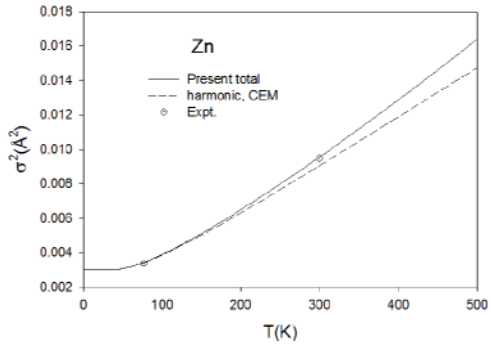

Fig. 5. Temperature dependence of the total MSRD of Zn compared to the harmonic one and to the experimetal values [16].

dependence of our calculated total MSRD of Zn compared to the harmonic one calculated by the correlated Einstein model and to the experimental values [16]. The temperature dependence of our calculated first and third cumulants of Zn is presented in Figs. 6 and 7, respectively, in comparison to experimental values [16]. It is shown that the calculated Morse potential presented in Fig. 2 is found to be in good agreement with the experimental result [28], and the EXAFS parameters calculated by present procedure, demonstrated in Figures 4-7 agree well with the experimental values [16] at 77 K and 300 K. Fig. 8 illustrates our calculated anharmonic contributions to the EXAFS phase of Zn at 77 K, 300 K and 500 K. It is seen that the phase shift due to anharmonicity is significant at 300 K and 500 K, but negligible at 77 K. Our calculated mean free path of the photoelectron of Zn

in the EXAFS process is illustrated in Fig. 9. All the above calculated parameters have been used for calculation of the EXAFS of Zn including anharmonic contributions. For XANES (X-ray Absorption Near Edge Structure) the multiple scattering is important, but for EXAFS the single scattering is dominant [29], and the main contribution to EXAFS is given by the first shell [7]. This is why for testing theory we present only the results for the first shell in single scattering. The generalization to the other shells is straighforward. EXAFS spectra according to Eq. (21) provide information on atomic number of each shell and on the thermodynamic parameters of the substance. The EXAFS calculated by using the famous FEFF code [1] of the University of Washington with harmonic model presented in Fig. 9a show no change at different temperatures 77 K, 300 K and 500 K,

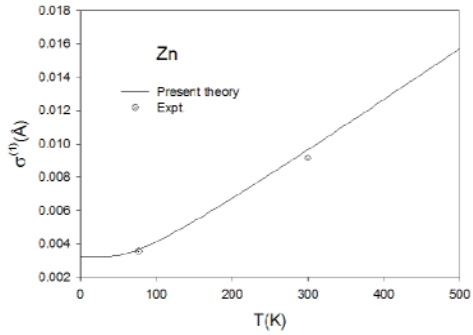

Fig. 6. Temperature dependence of the calculated first cumulant of Zn in comparison to experiment [16].

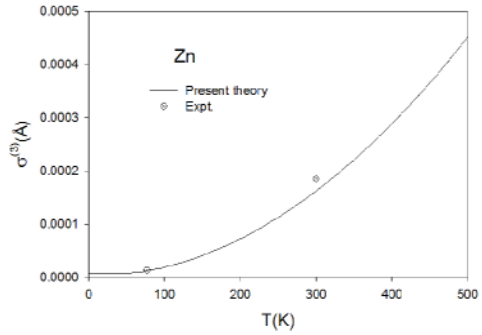

Fig. 7. Temperature dependence of the calculated third cumulant of Zn in comparison to experiment [16].

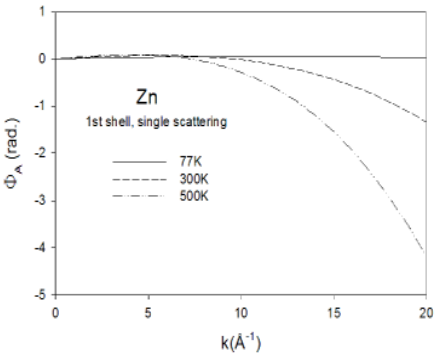

Fig. 8. Calculated anharmonic contributions to EXAFS phase of Zn at 77 K, 300 K and 500 K.

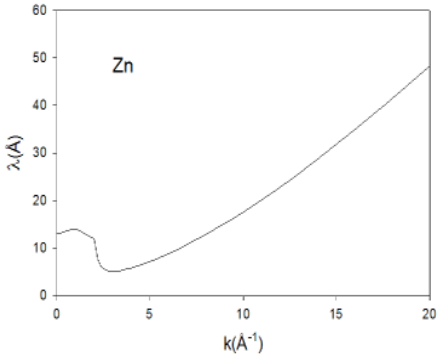

Fig. 9. Calculated mean free path of photoelectron of Zn in EXAFS process.

but those calculated by the present anharmonic procedure (Fig. 9b) contain significant phase changes at these temperatures, thus reflecting the phase shift effects appeared in the experiment shown in Fig. 1. Significant differences in phase and in amplitude of our calculated anharmonic EXAFS of Zn from those calculated by the harmonic model [1] are presented for T = 300 K (Fig. 10a) and for T = 500K (Fig. 10b). The anharmonic EXAFS spectra are attenuated and shifted to the left especially at high k-values. The attenuation

is caused by the anharmonic contribution to the amplitude presented in Fig. 4, and the phase shifts are caused by the anharmonic contributions to the phase presented in Fig. 8. The peaks of Fourier transform of the EXAFS provide information on the radius of atomic shells. Fourier transform magnitudes of EXAFS over the range 3.00 $\text{Å}^{-1} < k < 13.50\text{Å}^{-1}$ for Zn calculated by the FEFF code with harmonic model [1] (Fig. 12a) provide the same values of the first shell radius at different temperatures 77 K, 300 K and 500 K, but those calculated by present anharmonic theory (Fig. 12b) provide different values of the first shell radius which are shifted to the right as the temperature increases, thus reflecting apparently the effect of different information on the shell radius at the different high temperatures provided by the experiment shown in Fig. 2. Fourier transfom magnitudes of the EXAFS of Zn calculated by the present theory are compared to those calculated by the FEFF code and to experiment [16] for T = 77 K (Fig. 13a) and T = 300 K (Fig. 13b). They are found to be in good agreement with experiment [16]. The peaks are shifted to smaller distances by 0.05 Å at 300 K and 0.085 Å at 500 K in comparison to the harmonic model results. Thus providing apparently different structural information at the different high temperatures which must be treated for the harmonic model to describe the experimental results or to extract physical parameters from the experimental EXAFS data.

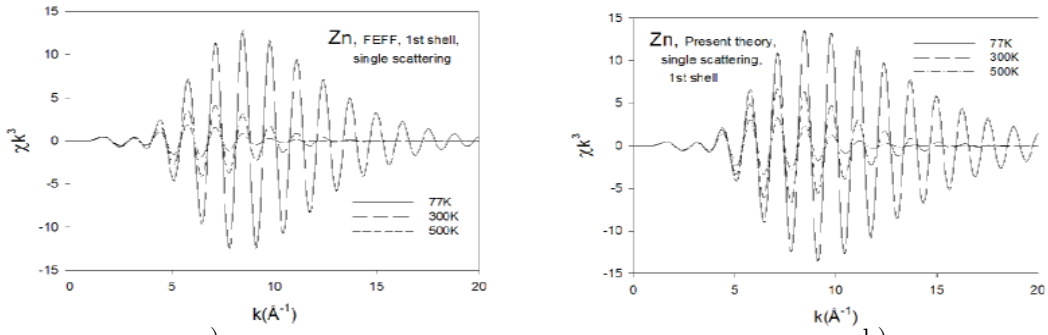

a) b)

Fig. 10. EXAFS calculated by harmonic FEFF with no phase shift (a) and those calculated by present anharmonic theory with different phase shifts (b) of Zn at 77 K, 300 K and 500 K.

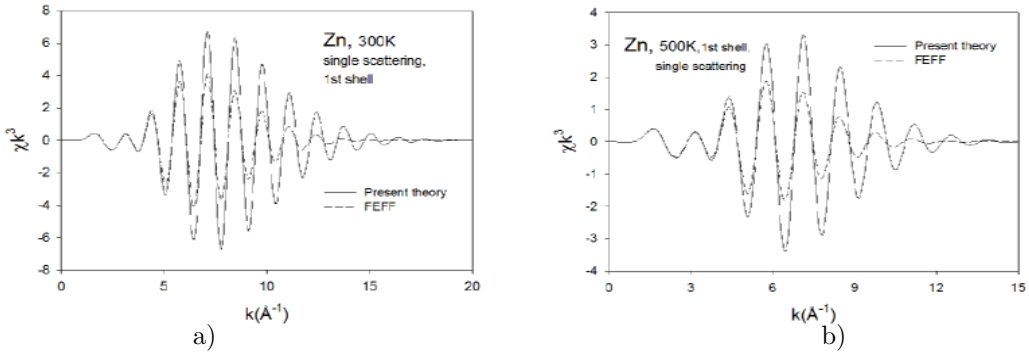

a) b)

Fig. 11. Comparison of EXAFS calculated by present anharmonic procedure with those calculated by harmonic FEFF [1] at 300 K (a) and at 500 K (b).

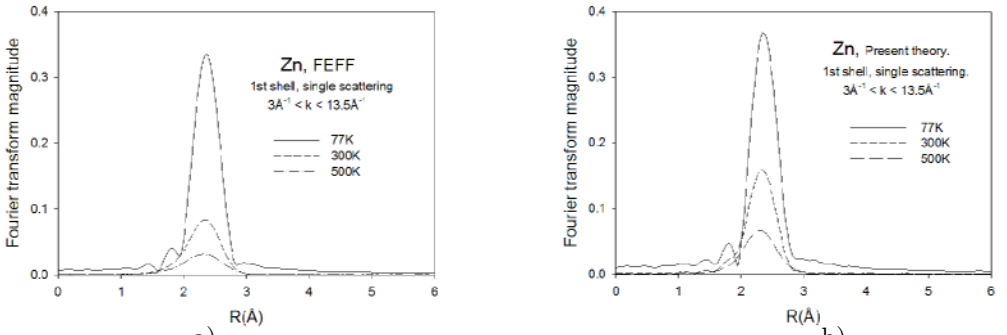

Fig. 12. Peaks of Fourier transform magnitudes of EXAFS for first shell of Zn calculated by FEFF code [1] with harmonic model provide the same shell radius at 77K, 300K and 500K (a), but those calculated by present anharmonic theory provide different shell radiuses at these temperatures (b) reflecting the experimental effect (Fig. 1).

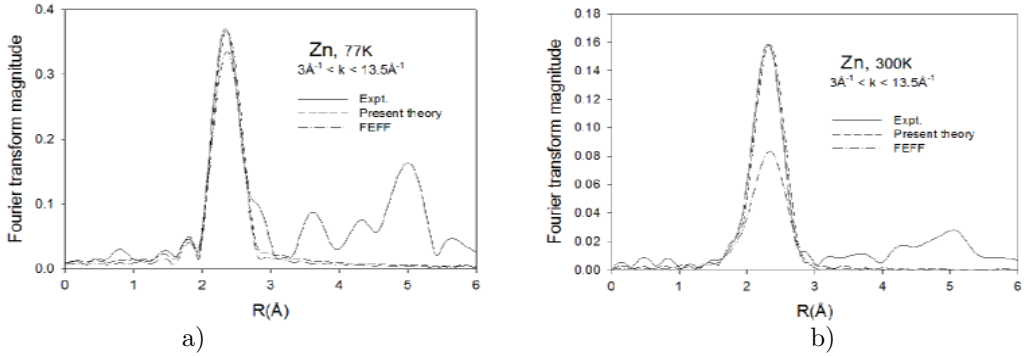

Fig. 13. Comparison of Fourier transform magnitude of EXAFS of Zn calculated by present anharmonic theory to those calculated by FEFF code [1] and to experiment [16] for T = 77 K (a) and T = 300 K (b).

IV. CONCLUSIONS

We have developed an anharmonic theory of EXAFS for hcp crystals based on the single shell approach and anharmonic correlated Einstein model. Our new development is derivation of expressions for the anharmonic contributions to the EXAFS amplitude and phase and its parameters. The total MSRD is the sum of the harmonic and the anharmonic contributions.

Advantages of the present procedure are as follows: the anharmonic contributions can be calculated and analyzed for any temperature and for any k-value; the present theory contains the results of the classical limit at high temperature and of the harmonic model at low temperature as its special cases; Morse potential parameters included in the anharmonic EXAFS and its parameters have been also calculated to fulfil the ab initio calculation procedure.

The good agreement between the calculated results and the experimental values shows the advantage and efficiency of this new theory for the calculation and analysis of the anharmonic EXAFS and its parameters of hcp crystals.

ACKNOWLEDGEMENTS

The authors thank Professor J. J. Rehr for allowance of using the FEFF code and Prof. R. R. Frahm for providing the experimental EXAFS data of Zn. One of the authors (N. V. Hung) thanks the BUGH Wuppertal for hospitality and financial support for his visit to Germany realizing cooperation work with Prof. R. R. Frahm and Dr. P. Keil in collecting experimental data. This work is also supported in part by the special research project of VNU-Hanoi QG.03.02 and the Basic Science Research Program.

REFERENCES

1. J. J. Rehr, J. Mustre de Leon, S. I. Zabinsky, and R. C. Albers, J. Am. *Chem. Soc.*, **113** (1991) 5135.
2. B. S. Clausen, L. Grabæk, H. Topsøe, L. B. Hansen, P. Stoltze, J. K. Nørskov, and O. H. Nielsen,*J. Catal.*, **141** (1993) 368.
3. E. D. Crozier, J. J. Rehr, and R. Ingalls, in *X-ray Absorption,* edited by D. C. Koningsberger and R. Prins Wiley, New York,1988) chapter **9**.
4. G. Bunker, *Nucl.&Instrum. Methods*, **207** (1983) 437.
5. J. M. Tranquada and R. Ingalls, *Phys. Rev. B*, **28** (1983) 3520.
6. L. Wenzel, D. Arvanitis, H. Rabus, T. Lederer, and L. Baberschke, *Phys. Rev. Lett.*, **64** (1990) 1765.
7. E. A. Stern, P. Livins, and Zhe Zhang, *Phys. Rev. B*, **43** (1991) 8850.
8. P. Fornasini, F. Monti, A. Sanson, *J. Synchrotron Rad.*, **8** (2001) 1214.
9. L. Tröger, T. Yokoyama, D. Arvanitis, T. Lederer, M. Tischer, and K. Baberschke, *Phys. Rev. B*, **49** (1994) 888.
10. N. V. Hung, R. Frahm, *Physica B*, **208** & **209** (1995) 91.
11. N. V. Hung, R. Frahm, and H. Kamitsubo, *J. Phys. Soc. Jpn.*, **65** (1996) 3571.
12. N. V. Hung, *J. de Physique* **IV** (1997) C2 : 279.
13. N. V. Hung and J. J. Rehr, *Phys. Rev. B*, **56** (1997) 43.
14. N. V. Hung, N. B. Duc, and R. R. Frahm, *J. Phys. Soc. Jpn.* **72** (2003) 1254.
15. N. V. Hung and D. X. Viet, *VNU-Jour. Science*, **19** (2) (2003) 19.
16. R. R. Frahm, unpublished.
17. M. Daniel, D. M. Pease, N. Van Hung, J. I. Budnick, *submitted to Phys. Rev. B*, (2003).
18. T. Yokoyama, T. Sasukawa, and T. Ohta, *Jpn. J. Appl. Phys.*, **28** (1989) 1905.
19. A. I. Frenkel and J. J. Rehr, *Phys. Rev. B*, **48** (1993) 583.
20. B. T. M. Willis and A. W. Pryor, *Thermal Vibrations in Crystallography*, Cambrige Univ. Press, London, 1975.
21. R. F. Feynman, *Statistical Mechanics* (Benjamin Reading, 1972).
22. T. Yokoyama, *Phys. Rev. B*, **57** (1998) 3423-3432.
23. A. V. Poiarkova, J. J. Rehr, *Phys. Rev.* B **59** (1999) 948-957.
24. J. J. Rehr, R. C. Albers, *Reviews of Modern Physics*, **72** (2000) 621-653.
25. Y. Okamoto, *et al.*, *J. Synchrotron Radiation*, **8** (2001) 1191-1199.
26. Paolo Fornasini, *et al.*, *J. Synchrotron Radiation*, **8** (2001) 1214-1220.
27. I. V. Pirog, *et al., J. Phys.: Condens. Matter*, **14** (2002) 1825-1832.
28. J. S. Slater, *Introduction to Chemical Physics* (McGraw-Hill Book Company, New York, 1939).
29. P. Rennert and N. V. Hung, *Phys. Statt. Solidi B*, **148** (1988) 49.

Received 3 December 2003